Magnetic dynamics with spin-transfer torques near the Curie temperature

Paul M. Haney and M. D. Stiles
Center for Nanoscale Science and Technology, National Institute of Standards and Technology, Gaithersburg, Maryland 20899-6202, USA

(Received 12 June 2009; revised manuscript received 26 August 2009; published 24 September 2009)

We use atomistic, stochastic Landau-Lifshitz-Slonczewski simulations to study the interaction between large thermal fluctuations and spin-transfer torques in the magnetic layers of spin valves. At temperatures near the Curie temperature T_C, spin currents measurably change the size of the magnetization (i.e., there is a *longitudinal* spin-transfer effect). The change in magnetization of the free magnetic layer in a spin valve modifies the temperature dependence of the applied field-applied current phase diagram for temperatures near T_C. These atomistic simulations can be accurately described by a Landau-Lifshitz-Bloch+Slonczewski equation, which is a thermally averaged mean-field theory. We use this equation to find the stability phase diagram of a ferromagnetic layer near its Curie temperature. Both the simulation and the mean-field theory show that a longitudinal spin-transfer effect can be a substantial fraction of the magnetization close to T_C.

DOI: 10.1103/PhysRevB.80.094418 PACS number(s): 75.47.−m, 75.40.−s, 75.75.+a

I. INTRODUCTION

Spin-transfer torque describes the interaction between the spin of itinerant, current-carrying electrons and the spins of the equilibrium electrons which comprise the magnetization of a ferromagnet. This torque results from the spin-dependent exchange-correlation electron-electron interaction, and leads to the mutual precession of equilibrium and nonequilibrium spins around the total spin. In spin valves with sufficiently high current density, spin-transfer torque can excite a free ferromagnetic layer to irreversibly switch between two stable configurations (typically along an easy axis, parallel, or antiparallel to an applied magnetic field), or to undergo microwave oscillations. Previous considerations of spin-transfer torque mostly focus on the *transverse* response of the magnetization to spin currents.[1–4] This is appropriate since the temperatures used in spin valve experiments are substantially below the Curie temperature T_C of the ferromagnets, so that longitudinal fluctuations can be ignored. Near T_C, one expects an interplay between the large thermal fluctuations and the nonequilibrium spin-transfer torque. Generally speaking, theories of critical phenomena in out-of-equilibrium systems have only recently been developed,[5,6] and there remain many open questions on this topic.

Even far from the Curie temperature, temperature plays an important role in quantitatively analyzing the dependence of the magnetic orientation on the applied field and applied current. The effect of finite temperature on spin dynamics in the presence of spin-transfer torque has been modeled with the macrospin approximation (fixed magnetization length) by adding a Slonczewski torque to the Langevin equation describing the stochastic spin dynamics,[7,8] and by solving the Fokker-Planck equation with the spin-transfer torque term added to the deterministic dynamics.[9] The Keldysh formalism provides a formal derivation of the stochastic equation of motion[10] for the nonequilibrium (i.e., current-carrying) system for a single spin of fixed magnitude. These treatments successfully describe the thermal characteristics of nanomagnets under the action of spin torques, such as dwell times and other details of thermally activated switching.

For materials such as GaMnAs, experiments are done near T_C, so that the *size* of the magnetization is substantially reduced from its low temperature value, and undergoes sizeable fluctuations. In this case, the relevance of a macrospin model is not clear. For field-driven dynamics, the longitudinal fluctuations near T_C can be treated in an approach that culminates in the construction of the Landau-Lifshitz-Bloch (LLB) equation,[11] which is an extension of the familiar Landau-Lifshitz equation with an additional longitudinal degree of freedom. Here, we extend this treatment by including spin-transfer torques, which can then be studied at temperatures near the Curie temperature.

The nature of the magnetic order at or above T_C is itself a difficult and complex problem. Models of magnetism near the phase transition generally fall between a disordered-local-moment (DLM) picture,[12,13] in which spins of constant magnitude occupy lattice sites and fluctuate in direction, and a pure Stoner model, in which all of the (itinerant) spins align and the transition is due to a vanishing moment magnitude. The fluctuating local band theory lies somewhere between these extremes;[14,15] there are a number of theories which can bridge the gap between the DLM and Stoner pictures of magnetic phase transition.[16,17] The inclusion of spin-transfer torque complicates this already complex problem. For example, the applicability of standard statistical mechanics techniques to this nonequilibrium system is not *a priori* clear.[10,18] For this reason, we adopt a rather pragmatic approach and extend the work of Garanin[11] to include the spin-transfer torque. This treatment is firmly rooted in the DLM end of the spectrum of phase transition models. We discuss the implications of this for the temperature dependence of the spin-transfer torque in the conclusion.

There are a number of other issues that complicate magnetic dynamics near T_C, including the temperature dependence of more basic magnetic properties such as magnetic damping and magnetocrystalline anisotropy, as well as the temperature dependence of the spin-transfer torque itself. We use an atomistic approach for the stochastic dynamics of a local-moment ferromagnet with the inclusion of spin-transfer torque. This "stochastic-local-moment model" is appropriate

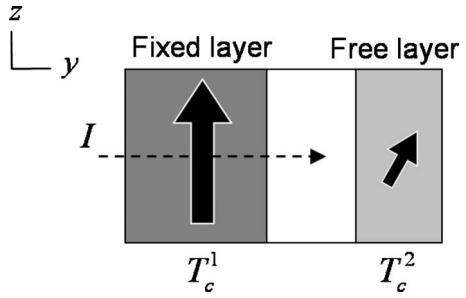

FIG. 1. Schematic of system, two ferromagnetic layers with different Curie temperatures. We suppose that $T_C^1 > T_C^2$.

for systems such as the dilute magnetic semiconductor GaMnAs. Our use of simple approximations for the temperature dependence of the magnetic anisotropy, demagnetization field, and damping allow us to focus in the interplay between thermal fluctuations and spin-transfer torque. We find that within this model, spin currents can change the *size* of the magnetization. We give an expression for this "spin-current longitudinal susceptibility," and propose an experimental scheme to measure this effect. The effect we describe is different than spin accumulation, which also changes the size of the moment. Here we describe the change in ordering in a disordered-local-moment model. Spin accumulation describes the change of the moment in Stoner-like models. There is spin accumulation in the conduction electrons in the model we consider, but it is negligible compared to the changes of the magnetization in the disordered-local moments.

We then construct a Landau-Lifshitz-Bloch +Slonczewski (LLBS) equation to describe both longitudinal fluctuations and spin-transfer torques (i.e., a single-domain model with variable magnetization length). Following Ref. 19, we verify the applicability of this single-domain model by comparing its results to the stochastic-local-moment model. We then analyze the single-domain model to find the applied field-applied current phase diagram for different temperatures. We find that critical switching currents are reduced by the same mechanism exploited in heat assisted magnetic recording, namely, the temperature-induced reduction in the magnetic anisotropy.[20] We also find that regions of the phase diagram which have been experimentally unattainable become relevant at high temperatures. The dependence of critical currents on temperature in these regions can provide quantitative details about the temperature dependence of spin-transfer torque.

II. METHOD

To study the interplay between temperature and spin-transfer torque, we treat a temperature-independent spin-current flux incident on a free layer at a variable temperature. This approach is appropriate for spin valves with fixed-layer magnetizations having Curie temperatures T_C^1 much greater than the variable temperature and the Curie temperature T_C^2 of the free layer (see Fig. 1). We choose the spin-transfer torque to have the form

$$H_I(\mathbf{S}_i \times \mathbf{S}_i \times \hat{z}), \tag{1}$$

where H_I parameterizes the spin-transfer torque: $H_I = -Ip\mu_B/\mu_0 e\gamma M_s^0 \ell A$, where I is the applied current, p is the spin polarization of the current, M_s^0 is the zero-temperature magnetization, ℓ is the free layer thickness, A is the transverse layer area, and e is the (negative) electron charge. This approximation assumes that the incoming spin current acts uniformly on the free layer magnetization and is based on two expectations—that the spin-transfer torque is largely interfacial but the exchange interaction in the direction of current flow is strong enough to minimize fluctuations in that direction. Substantial spatial and temporal inhomogeneities in the magnetization should induce rather irregular spatial patterns in the spin currents carried by propagating states. This will lead to large dephasing effects, so that the total spin current should rapidly decay away from the interface as in the conventional picture of spin-transfer torques.[3] In addition, in this temperature regime, and for thin layers ($\approx$3 nm), magnetic nonuniformities in the direction transverse to current flow should be more substantial than nonuniformities *along* the current flow resulting from a localized spin-transfer torque. This assumption is most applicable to the DLM model of a ferromagnet near its transition temperature. If a Stoner type of transition is assumed, then there is a much weaker but uniform exchange field, and the assumption that all of the transverse spin current is absorbed is not necessarily as well founded.

A. Model I: Stochastic local moment

We adopt three approaches to model the system. The first is an atomistic lattice model of normalized spins $\mathbf{S}$, which we treat with a stochastic Landau-Lifshitz (SLL) equation. (As discussed in the introduction, the use of temperature-independent spins in the lattice makes this model more relevant to a disordered-local-moment model of the magnetic phase transition than to a Stoner type phase transition.) We include nearest-neighbor Heisenberg coupling with exchange constant J, and an easy-axis anisotropy field of magnitude H_{an} in the $\hat{z}$ direction. To model the temperature dependence of the anisotropy, we make the ansatz that the magnitude of anisotropy at temperature T is proportional to the reduced magnetization $m(T) = M_s(T)/M_s^0$,

$$H_{an}(T) = H_{an}(T=0)m(T), \tag{2}$$

so that the anisotropy field on spin i is given by $H_{an}^i(T) = H_{an}(T=0)\overline{|\mathbf{S}|}S_i^z$, where the bar indicates a spatial average. This choice gives an effective (i.e., spatially and thermally averaged) anisotropy that varies as $m^3(T)$, which is the behavior typically ascribed to uniaxial anisotropies.[21] We model the demagnetization field of the thin layer by a hard-axis anisotropy field with magnitude H_d in the $\hat{y}$ direction. We take the demagnetization field to be uniform on all spins and given by $H_d^i(T) = -H_d(T=0)\overline{S^y}\hat{y}$. This form of the hard-axis field ensures that $H_d \sim M_s(T)$, and roughly captures the nonlocal nature of the field. This form also simplifies the numerics. Finally, we include an applied field H_{app} in the $\hat{z}$ direction. The Hamiltonian for spin i is then

$$H_i = J\sum_{j\in \text{n.n.}} \mathbf{S}_i\cdot\mathbf{S}_j + \mu_B\mu_0\left(\frac{H_{\text{an}}(T=0)|\overline{\mathbf{S}}|}{2}(S_i^z)^2 - H_{\text{d}}(T=0)S_i^y\overline{(S^y)} + H_{\text{app}}S_i^z\right), \quad (3)$$

where the sum in the first term is over nearest neighbors, μ_B is the Bohr magneton, and μ_0 is the permeability of free space. To model nonzero temperatures, we add damping α and a stochastic field $\mathbf{H}_{\text{fl}}$ to the equation of motion implied by Eq. (3), with the standard statistical properties,

$$\langle H_{\text{fl}}^i(t)\rangle = 0, \quad (4)$$

$$\langle H_{\text{fl}}^i(t)H_{\text{fl}}^j(t')\rangle = \frac{\alpha}{1+\alpha^2}\frac{2k_BT}{\gamma\rho}\delta_{ij}\delta(t-t'), \quad (5)$$

where i,j are the Cartesian components of the field, k_B is the Boltzmann constant, ρ is the magnetic moment on each lattice site, and γ is the gyromagnetic ratio. We numerically integrate the equation of motion using a second-order Heun scheme.[22] We add a Slonczewski-like spin-transfer torque term to the equation of motion for the ith spin, which is given finally as

$$\dot{\mathbf{S}}_i = -\gamma\mu_0[\mathbf{S}_i\times(\mathbf{H}_{\text{eff}}+\mathbf{H}_{\text{fl}}) - \alpha(\mathbf{S}_i\times\mathbf{S}_i\times\mathbf{H}_{\text{eff}}) + H_I(\mathbf{S}_i\times\mathbf{S}_i\times\hat{z})]. \quad (6)$$

The effective magnetic field is given by $\mathbf{H}_{\text{eff}}=H_{\text{app}}\hat{z}+H_{\text{an}}\overline{|\mathbf{S}|}S_i^z\hat{z}-H_{\text{d}}\overline{(S^y)}\hat{y}+J/(\mu_B\mu_0)\Sigma_{j\in\text{n.n.}}\mathbf{S}_j$. We use both a bulk geometry consisting of a $N=48^3$ periodic array of spins in three dimensions (simple cubic lattice), and a layer geometry with an array of $100\times100\times15$ spins. We employ the bulk geometry in comparing the stochastic model behavior with predictions from mean-field theory, and the layer geometry for studying the effect of spin current on magnetization size.

B. Model II: Single domain with variable size

For our second approach, we derive a thermally averaged version of the stochastic-local-moment model, where nearest-neighbor exchange is replaced by its mean-field value. In the absence of spin-transfer, the resulting equation is known as the Landau-Lifshitz-Bloch equation. The details of the derivation with the inclusion of spin-transfer torque follow closely those in Ref. 11, so we omit them here. The final "Landau-Lifshitz-Bloch-Slonczewski" equation (which, for simplicity we will refer to as the "single-domain model") takes the form

$$\dot{\mathbf{m}} = -\gamma\mu_0\left[(\mathbf{m}\times\mathbf{H}_{\text{eff}}) + \frac{2k_BT}{J_0m^2}\mathbf{m}\cdot(\alpha\mathbf{H}_{\text{eff}}+H_I\hat{z})\mathbf{m} - \frac{1}{m^2}\left(1-\frac{k_BT}{J_0}\right)\mathbf{m}\times\mathbf{m}\times(\alpha\mathbf{H}_{\text{eff}}+H_I\hat{z})\right], \quad (7)$$

with an effective field given by

$$\mathbf{H}_{\text{eff}} = H_{\text{app}}\hat{z} + H_{\text{an}}m^2m_z\hat{z} - H_{\text{d}}m_y\hat{y} - \frac{M_{\text{s}}^0}{2\chi}\left(\frac{m^2}{m_e^2}-1\right)\mathbf{m}, \quad (8)$$

where M_{s}^0 is the zero-temperature saturation magnetization, $\mathbf{m}=\mathbf{M}/M_{\text{s}}^0$ is the dimensionless magnetization with magnitude between zero and one, $m_e(T)$ is the zero field, zero current equilibrium magnetization: $m_e(T)=B(J_0/k_BT)$, where B is the Brillouin function. $\chi(T)$ is the longitudinal susceptibility: $\chi(T)=M_{\text{s}}^0(\partial m_e(T)/\partial H_{\text{app}})$. J_0 is the zero wave-vector component of the Fourier transformed exchange. The spin-transfer torque is parameterized by H_I, as described in the previous section. The double cross product in Eq. (7) is the familiar Landau-Lifshitz damping term, which describes the relaxation of the magnetization *direction* to the nearest energy minimum. The term parallel to $\mathbf{m}$ distinguishes the LLB equation from the Landau-Lifshitz equation. This longitudinal term describes the relaxation of the *size* of the magnetization to its steady state value, which is determined by the temperature, applied fields, and applied currents.

The detailed dependence of the magnetic anisotropy on temperature is generally material specific. We use the thermal average of the anisotropy and demagnetization fields as described in Eq. (3) of the stochastic-local-moment model. This results in anisotropy and demagnetization fields which depend on temperature through their m dependence, and vary as $m^3(T)$ and $m(T)$, respectively. The magnetic exchange J_0 can also depend on temperature. This dependence is stronger for ferromagnets with indirect exchange interactions (such as GaMnAs, where the magnetic interactions are mediated by hole carriers), and weaker for local-moment systems with direct exchange (such as Fe). For simplicity we treat J_0 as temperature-independent.

Finally we consider the standard Landau-Lifshitz equation with a reduced but fixed saturation magnetization. We find in Sec. III D that it is possible to appropriately modify the damping coefficient in a standard Landau-Lifshitz approach so that the phase diagram it predicts agrees qualitatively with those predicted by the more complicated models.

III. RESULTS

A. Longitudinal spin-current susceptibility

In transition metal ferromagnets, longitudinal spin transfer is typically quite small compared to the magnetization and has a negligible effect on the magnetization dynamics. (As discussed in the introduction, longitudinal spin transfer may be due to spin accumulation, or transverse-spin-transfer-induced ordering of local moments; the latter case is considered here.) However, for temperatures close to the Curie temperatures, the longitudinal spin transfer can be a sizeable fraction of the magnetization and can significantly affect the dynamics.

For the single-domain model, it is straightforward to show from Eq. (7) that the change in the magnetization in the presence of spin current is

$$\delta m(I,T) = \frac{H_I}{M_{\text{s}}^0}\frac{\chi(T)}{\alpha}. \quad (9)$$

In order to verify that this expression is also valid for the stochastic-local-moment model, we use a lattice of 100

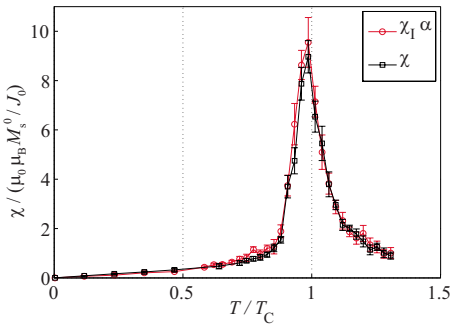

FIG. 2. (Color online) The magnetic field and spin-current susceptibility versus temperature for the stochastic Landau-Lifshitz equation in the layer geometry. The spin-current susceptibility is multiplied by α. The error bars indicate statistical uncertainty (one standard deviation). In the plot, χ is rescaled by $\mu_0 \mu_B M_s^0 / J$.

$\times 100 \times 15$ spins and calculate the susceptibilities. The results are shown in Fig. 2, which shows the longitudinal susceptibility to magnetic field and spin current. (In Fig. 2 χ is divided by a combination of factors based on the dimensionless variables we use: the magnetic field is scaled by the exchange field $J_0/\mu_B\mu_0$, and the magnetization is scaled by M_s^0.) In the simulation, the spins' polar angle is initialized to a uniform distribution between $\theta=0$ and $\theta=\theta_{\max}$, where $\theta_{\max}$ is chosen so that the initial spins' average is equal to the equilibrium value. We allow the system to relax to steady state, and find the value of the magnetization and its fluctuations by finding the average and standard deviation over an interval of time (the appropriate time interval is temperature dependent). The fluctuations lead to the statistical uncertainty shown in Fig. 2.

The spin-current susceptibility χ_I is defined as $\chi_I = M_s^0(\partial m/\partial H_I)$. We find that χ and $\chi_I\alpha$ agree to within numerical uncertainty, demonstrating that Eq. (9) (derived using the single-domain model) *also* accurately describes the behavior of the stochastic-local-moment model.

The change in magnetization should be measurable. The fractional change in the magnetization compared to the zero-temperature saturation magnetization is

$$\delta m = \left(\frac{p\mu_B}{e\gamma\mu_0 \ell A (M_s^0)^2}\right)\left(\frac{\chi(T)}{\alpha}\right) I. \tag{10}$$

For $T/T_C=0.95$, so that $(\chi \cdot J_0/\mu_0\mu_B M_s^0)=7$ (from Fig. 2), and with an exchange field of $J_0/\mu_B\mu_0=1.2\times10^8$ A/m (which corresponds to a T_C of 150 K in a cubic nearest-neighbor Heisenberg model), $M_s^0=10^6$ A/m, $I/A=10^{11}$ A/m^2, $p=0.5$, $\alpha=0.01$, and $\ell=3$ nm gives a change compared to the zero-temperature value of $\delta m=5\%$. Since the magnetization is reduced to approximately 20% of its zero-temperature value at $T/T_C=0.95$, the fractional change in the magnetization due to the current is approximately 25%.

A notable aspect of this longitudinal spin transfer is that the size of the magnetization can either be increased or decreased according to the direction of current flow. For parallel average magnetizations, with electron flow from fixed to free layer, the free layer moment *increases*, while electron flow in the opposite direction *decreases* the free layer moment. This contrasts with current-induced Joule heating, which always decreases the magnetization.

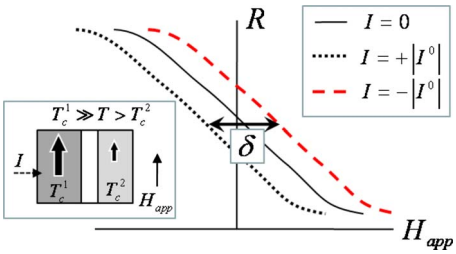

FIG. 3. (Color online) Experimental scheme for detecting longitudinal spin transfer: for $T_C^1 \gg T > T_C^2$, an applied field H_{app} changes the resistance R via the magnetoresistance effect. The application of a positive and negative current density of magnitude I^0 shifts $m(H_{app})$ in the positive and negative direction, respectively, via longitudinal spin transfer. The $R(H_{app})$ curves therefore shift to the positive and negative directions.

This distinction can be exploited to probe the longitudinal spin transfer by using the experimental scheme shown in Fig. 3. We consider the case where $T_C^1 \gg T > T_C^2$. We choose sign conventions such that a positive H_{app} aligns with the fixed layer, and a positive current represents electron flow from fixed to free layer. In the absence of an applied current ($I=H_I=0$, black line in Fig. 3), the application of a magnetic field will partially order the free layer to align or antialign with the fixed layer. This should cause the resistance R of the device to change in some way, according to the giant magnetoresistance effect and magnetic order induced in the free layer (the detailed dependence of R on H_{app} is not important here). If a positive current I^0 is applied, then the longitudinal spin transfer induces partial ordering of the free layer, so that $m(H_{app}=0)=+\chi_I H_{I^0}/M_s^0$. Then the curve of $m(H_{app})$, and therefore the curve $R(H_{app})$ is simply shifted by $+\chi_I H_{I^0}/\chi$ (the black dotted curve in Fig. 3). If a negative current density $-|I^0|$ is applied, then $m(H_{app}=0)=-\chi_I H_{I^0}/M_s^0$ and the $m(H_{app})$ and $R(H_{app})$ curves are shifted by $-\chi_I H_{I^0}/\chi$ (red dashed curve in Fig. 3). This *rigid shift* represents a unique signature of longitudinal spin transfer. (Note that a simple current-induced change in R at finite applied field may be due to transverse spin transfer, so that this rigid shift is a key signature to the longitudinal spin transfer.)

Using the same parameters as before, we estimate a total shift $\delta=2\chi_I H_{I^0}/\chi$ between $R(H_{app})$ for positive and negative current to be on the order of 8×10^5 A/m. (≈ 1 T) Eq. (10) indicates that materials with small exchange field (or small T_C), and those that can support large current densities show the effect most strongly. This suggests that weak metallic ferromagnets such as Gd ($T_C=300$ K), and Fe alloys such as FeS_2 and $FeBe_5$ ($T_C=270$ K) (Ref. 23) may be good candidates for free layer material.

B. Stochastic local moment vs single domain model

The single-domain model represents a vast simplification to the stochastic-local-moment model. The degree to which the single-domain model reproduces the behavior of the

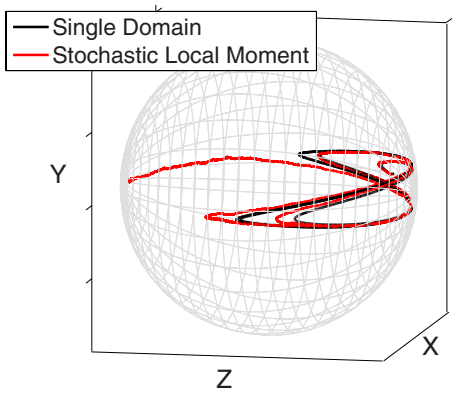

FIG. 4. (Color online) Single-domain (black line) and stochastic-local-moment [red (gray) line] trajectories for $T'=0.24$ The single-domain model shows persistent oscillations, while the stochastic-local-moment model undergoes switching. The hard axis and easy axis are in the $\hat{y}$ and $\hat{z}$ directions, respectively.

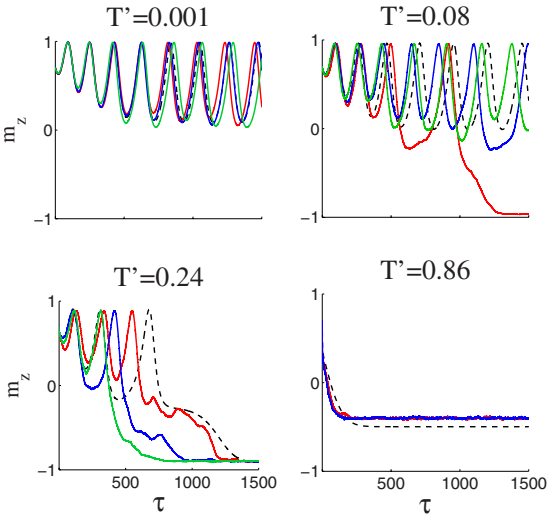

FIG. 5. (Color online) Comparison of the ($\hat{z}$ component) magnetization time evolution with spin-transfer torque for the atomistic stochastic simulation and the LLB+Slonczewski equation for various reduced temperatures $T'=T/T_C$. The dashed line gives the LLB +Slonczewski trajectory, while the solid lines show various realizations of the stochastic trajectory. The dimensionless time τ is given by $\tau=(\gamma J/\mu_B)t$.

stochastic-local-moment model is not *a priori* obvious, and is the subject of this section. We consider a current-induced magnetic excitation for the bulk lattice geometry at various temperatures. The average magnetization is initialized at a 45° angle with respect to the $+\hat{z}$ direction (the individual spins' initial direction is distributed uniformly within 3° in the θ, ϕ direction about $\theta=45°$, $\phi=0°$). The spin-transfer torque is applied to excite the magnetization away from the $\hat{z}$ direction. In our numerics, we rescale time t to $\tau=(\gamma J/\mu_B)t$, which rescales the magnetic fields H_{eff} by the exchange field $H_{\text{ex}}=J/\mu_0\mu_B$. Dimensionless fields are denoted by lowercase: $h_{\text{app}}=H_{\text{app}}\mu_0\mu_B/J$, etc. The dimensionless spin torque is denoted by j_{app}, where $j_{\text{app}}=H_I\mu_0\mu_B/J$. The parameters used are an applied field of $h_{\text{app}}=0.0001$, a demagnetization field of $h_{\text{d}}=0.01$, a current of $j_{\text{app}}=-0.0002$, and damping of $\alpha=0.1$ (the artificially high damping was chosen to allow the numerical simulation of the switching to be carried out in a reasonable time). The time step used for the numerical integration is $d\tau=0.0002$. We vary the temperature T, and present results in terms of the scaled temperature $T'=T/T_C$.

As we increase temperature, we obtain trajectories of varying complexity. Figure 4 shows the trajectories obtained with the single-domain model and a realization of the stochastic-local-moment (the spatial average of the stochastic-local-moment model is shown), for $T'=0.24$. Figure 5 shows the temperature dependence of the trajectories ($\hat{z}$ component shown) obtained with the single-domain model with several realizations of the stochastic-local-moment model. For this range of parameters, the magnetic dynamics evolves from steady oscillations to current-induced switching as the temperature is increased. Generally, the level of correspondence between the two is qualitatively good, although it varies between different realizations of the stochastic dynamics. We can conclude from this data that the single-domain model qualitatively captures the features of the full stochastic-local-moment model.

The trajectories for $t=0.08$ indicate that a realization of stochastic dynamics can exhibit the crossover from precession to stable switching, whereas at this temperature the trajectory obtained with the single-domain model shows only oscillations. This illustrates an important distinction between the stochastic local moment and single-domain models. The single-domain model describes the thermally averaged magnetization, derived using an assumed probability distribution function (in this case, a distribution function most appropriate for temperatures well above and below energy barriers). For this reason, the single-domain model does not contain information about fluctuations, and in particular does not capture stochastic switching over the energy barrier. The fluctuations may be obtained by solving the Fokker-Planck equation, or by supplementing the single-domain model with stochastic fields, as done in Ref. 24.

C. Applied field-applied current phase diagram

We next study the stability of the single-domain model. Both high temperatures and the longitudinal degree of freedom change the applied field-applied current phase diagram of the free magnetic layer. Figure 6 shows the generic topology for regions of stability for the parallel ("P," or $+\hat{z}$ direction) and antiparallel ("AP," or $-\hat{z}$ direction) fixed points. We focus on the stability of the AP configuration for positive applied fields (the dashed boundary in the upper half-plane of Fig. 6. We first briefly describe the main qualitative features before providing a mathematical description. For applied fields between $h_{\text{an}}m^3$ and $h_{\text{an}}m^3+h_{\text{d}}m$, the stability boundary is a horizontal parabola, while for other values of applied field, the stability boundary is linear with slope $1/\alpha$. For applied fields with magnitude less than $h_{\text{an}}m$, there is hysteresis in the current switching. For $T=0$, this phase diagram reduces to the known form found experimentally.[25] As T increases, the size of the hysteretic region (and the switching current) decreases. Also the range of field with the parabolic boundary decreases, and the outer edge of the parabola

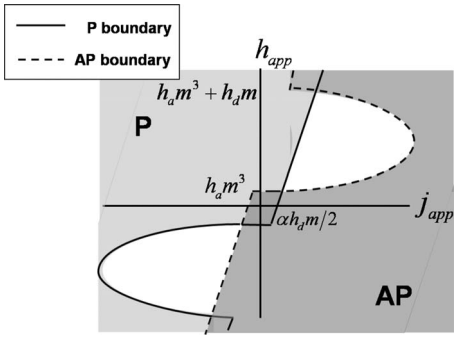

FIG. 6. Schematic of parallel/antiparallel stability versus applied field and applied current. The hysteretic box near the origin and the fully unstable regions (white parabolic shapes) contract in size with increasing temperature.

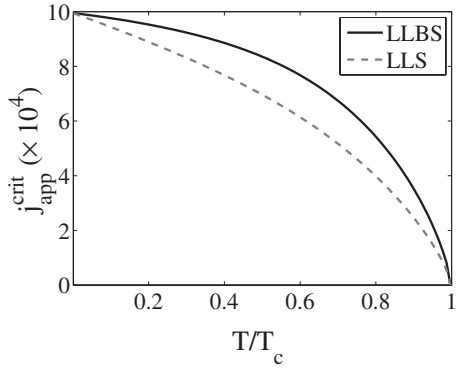

FIG. 7. Critical current versus temperature for LLBS and LLS equations. The parameters are: $h_{app}=-0.001$, $h_d=0.01$, $h_{an}=0.0001$. Recall that all fields are scaled by the exchange field.

gets pulled in closer to 0. For sufficiently high temperatures, this parabolic stability boundary should be experimentally accessible.

A quantitative description of the phase diagram follows from Eq. (7). We determine the stability of fixed points using the standard method of linearizing Eq. (7) about a fixed point and finding parameter-dependent eigenvalues λ. A positive real part of λ indicates a loss of stability. This analysis leads to the following condition for instability of the antiparallel configuration [where it should be noted that m depends on j_{app} through $m=m_e+\tilde{\chi}(h+\frac{j_{app}}{\alpha})$, and $\tilde{\chi}$ is the rescaled susceptibility, given by $\tilde{\chi}=\chi(J_0/\mu_0\mu_B M_s^0)$]:

$$\mathrm{Re}\left\{ j_{app}^{crit} + \alpha\left[h + h_{an}m^3 + \frac{h_d}{2}m\frac{1-T'}{1-3T'} - \frac{m}{2\tilde{\chi}}\left(1-\frac{m^2}{m_e^2}\right)\frac{2T'}{1-3T'}\right] - \frac{m\sqrt{-(h+h_{an}m^3)(h+h_{an}m^3+h_d m)}}{1-3T'}\right\} = 0.$$

This leads to a cubic equation for j_{app}^{crit}. Assuming $m_e \gg \tilde{\chi}(h+\frac{j_{app}}{\alpha})$, and expanding to 0th order in $\tilde{\chi}$ leads to an approximate, closed form for j_{app}^{crit}. Again we distinguish between different regimes of applied field. For $h \notin [h_{an}m^3, h_{an}m^3+h_d m]$

$$j_{app}^{crit} = \alpha\left(h + \frac{h_d}{2}m_e + h_{an}m_e^3\frac{1-3T'}{1-T'}\right), \tag{11}$$

where again m_e is the equilibrium magnetization in the absence of applied field and applied current. Equation (11) shows that the slope of the boundary is temperature independent, and is given by $1/\alpha$ (the intrinsic damping α is assumed to be temperature independent). The temperature independence of the slope follows from the fact that the spin-transfer torque increases like $1/m(T)$, but the effective damping rate also increases as $1/m(T)$. The intercepts of this boundary line are temperature dependent due to the temperature dependence of m. The contribution from the easy-axis anisotropy field has an additional temperature dependence, but the magnitude of this field is much smaller than the demagnetization field, so it does not play an important role. The critical current at zero field is reduced by $m(T)$ because of the reduction in the demagnetization field. This is important because the demagnetization field is usually larger than applied fields, and is therefore the primary impediment to current-induced switching. Its reduction through increased temperature offers a route to reduced critical switching currents.

For $h_{an}m^3 < h < h_{an}m^3 + h_d m$, a very large spin torque is required to stabilize the AP configuration. The values of current for which the AP configuration is stabilized are much higher than those attainable experimentally, so that for this range of fields the AP configuration is not seen.[26] The approximate critical current along the AP stability boundary is

$$j_{app}^{crit} = \frac{m_e\sqrt{h(h_d m_e - h)}}{1-T'}. \tag{12}$$

The outer boundary of the parabolic stability line is reduced at high temperature, and this reduction can also be traced back to the reduced magnetic anisotropy. For low temperatures, the application of spin-transfer torques results in an elliptical precession mostly in the easy plane about the $-\hat{z}$ fixed point. To stabilize the AP configuration in this regime, the spin-transfer torque must overcome the *precessional* torque (usually, the spin-transfer torque must overcome the much weaker *damping* torque). Assuming $h=h_d m/2$ for definiteness, the precessional torque decreases with T as $h_d m(T)$, while the spin-transfer torque increases like $1/m$. This implies a value for the maximum reach of the parabola of $j_{app} = m^2(T)h_d/[2(1-T)]$. Plugging in typical values for material parameters (the same used in Sec. III A) leads to a critical current of 10^{12} A/m^2 for $T=0.95T_C$. This is an order of magnitude smaller than the zero-temperature case. The behavior of this critical current versus temperature at a fixed applied field is shown in Fig. 7. (Solid line gives LLBS result.) It should also be noted that the stochastic trajectories (shown in Fig. 5) indicate that thermal fluctuations can effectively drive the system out of the precessional state and into the static antiparallel configuration.

D. Comparison with Landau-Lifshitz-Slonczewski

The Landau-Lifshitz-Slonczewski (LLS) equation can be modified to emulate the single-domain model discussed so far [i.e., the Landau-Lifshitz-Bloch-Slonczewski (LLBS) equation]. Based on the qualitative behavior of the LLBS equation, a suitable form for a temperature dependent LLS equation for a nanomagnet of reduced magnetization length m and orientation $\hat{n}$ is

$$\dot{\hat{n}} = -\gamma\mu_0\left(\hat{n}\times\mathbf{H}_{\mathrm{eff}} - \frac{\alpha}{m}\hat{n}\times\hat{n}\times\mathbf{H}_{\mathrm{eff}} - \frac{H_I}{m}\hat{n}\times\hat{n}\times\hat{z}\right),$$

where $\mathbf{H}_{\mathrm{eff}}=\mathbf{H}_{\mathrm{app}}-mH_{\mathrm{d}}n_y\hat{y}+m^3H_{\mathrm{an}}n_z\hat{z}$, and the temperature dependence is contained entirely in $m(T)$. The differences between this LLS equation and the LLBS equation are quantitative (as opposed to qualitative) in nature. One difference is in the dependence of the critical current on temperature for $h_{\mathrm{an}}m^3<h<h_{\mathrm{an}}m^3+h_{\mathrm{d}}m$. Figure 7 shows the prediction based on the LLS equation.

The LLS equation neglects the longitudinal spin transfer and applied-field susceptibility, which are responsible for dynamically changing the size of the magnetization (and therefore the size of the effective fields) during a switching event, or other magnetization dynamics. However, Fig. 7 shows qualitative agreement between the critical currents found in both LLBS and LLS models. This is indicative of the fact that for the applied field-applied current phase diagram, the spin-current and applied-field longitudinal susceptibilities play a role that is secondary to the more pronounced effects of temperature reduced anisotropies.

IV. DISCUSSION

Spin-transfer torques can affect the longitudinal fluctuations of a ferromagnet near its critical temperature. To investigate these effects, we studied an atomistic, stochastic Landau-Lifshitz-Slonczewski simulation at high temperatures. We find that there is a longitudinal spin-transfer effect, and estimate that at temperatures near T_{C}, spin currents can measurably change the size of the magnetization. We then supplemented the Landau-Lifshitz-Bloch equation with a Slonczewski torque term, and verified that this model captures the qualitative features of the stochastic simulations. We showed that the applied field-applied current phase diagram undergoes large changes in the presence of high temperatures, and that these changes may be useful for reducing critical switching currents and for studying the detailed behavior of the temperature dependence of the spin-transfer torque. It should be emphasized that these results are predicated on a disordered-local-moment model of a ferromagnetic phase transition. This model leads to an effective damping that increases with temperature as $1/m(T)$, which effectively counteracts the similar $1/m(T)$ increase in the magnitude of spin-transfer torque. Materials that undergo a Stoner transition should also have a $1/m(T)$ dependence for the spin-transfer torque, but a different temperature dependence for damping. Such materials should therefore behave differently than the model considered here.

The experimental system relevant for the effects we describe (shown schematically in Fig. 1) should be relatively straightforward to fabricate. Jiang *et al.* considered a similar system,[27] although that work dealt with other issues such as the ferrimagnet compensation point for magnetization and total angular momentum. By considering simpler ferromagnets with different Curie temperature, the role of temperature may be more easily inferred. It is of course necessary to account for Joule heating in assessing the detailed temperature dependence of the spin-transfer torque. However recent experiments on domain wall motion illustrate the feasibility of compensating for this effect.[28] On the other hand, experiments conducted at fixed current with varying ambient temperature and applied fields may offer a more straightforward route to observing the longitudinal spin-transfer effect.

There have been experiments performed on dilute magnetic semiconductor spin valves.[29,30] In this case it was recognized that the temperature dependence of the magnetic anisotropy was key to interpreting the measured switching currents. However, the additional complication of strong spin-orbit coupling in GaMnAs makes direct application of the theory presented here problematic: the spin-orbit coupling invalidates the picture of the spin-transfer torque as being equal to the imbalance between incoming and outgoing spin current.[31] There have additionally been many experiments with dilute magnetic semiconductors dealing with domain wall motion, where thermal effects play an important role in even the qualitative aspects of the domain wall behavior.[28] There are additional challenges associated with extending this work from spin valves to continuous magnetic textures. Among these is the renormalization of the exchange interaction associated with the coarse graining of the magnetization, which becomes more important at higher temperatures.[32] In addition, the crucial role played by the demagnetization field in intrinsic domain wall pinning implies that the finite temperature treatment of the demagnetization field must also be handled more carefully. For these reasons the spin valve geometry may provide greater experimental control and admit a simpler theoretical description.

[1] J. C. Slonczewski, J. Magn. Magn. Mater. **62**, 123 (1996).
[2] L. Berger, Phys. Rev. B **54**, 9353 (1996).
[3] M. D. Stiles and A. Zangwill, Phys. Rev. B **66**, 014407 (2002).
[4] A. Brataas, G. E. W. Bauer, and P. J. Kelly, Phys. Rep. **427**, 157 (2006).
[5] A. Mitra, S. Takei, Yong Baek Kim, and A. J. Millis, Phys. Rev. Lett. **97**, 236808 (2006).
[6] D. E. Feldman, Phys. Rev. Lett. **95**, 177201 (2005).
[7] Z. Li and S. Zhang, Phys. Rev. B **69**, 134416 (2004).
[8] J. Xiao, A. Zangwill, and M. D. Stiles, Phys. Rev. B **72**, 014446 (2005).
[9] D. M. Apalkov and P. B. Visscher, Phys. Rev. B **72**, 180405(R)

(2005).
[10] A. S. Núñez and R. A. Duine, Phys. Rev. B **77**, 054401 (2008).
[11] D. A. Garanin, Phys. Rev. B **55**, 3050 (1997).
[12] J. Hubbard, Phys. Rev. B **23**, 5974 (1981).
[13] H. Hasegawa, J. Phys. Soc. Jpn. **49**, 178 (1980).
[14] H. Capellmann, J. Phys. F: Met. Phys. **4**, 1466 (1974).
[15] V. Korenman, J. L. Murray, and R. E. Prange, Phys. Rev. B **16**, 4032 (1977).
[16] J. B. Staunton and B. L. Gyorffy, Phys. Rev. Lett. **69**, 371 (1992).
[17] V. Antropov, Phys. Rev. B **72**, 140406(R) (2005).
[18] A. Mitra and A. J. Millis, Phys. Rev. B **77**, 220404(R) (2008).
[19] O. Chubykalo-Fesenko, U. Nowak, R. W. Chantrell, and D. A. Garanin, Phys. Rev. B **74**, 094436 (2006).
[20] R. E. Rottmayer, S. Batra, D. Buechel, W. A. Challener, J. Hohlfeld, Y. Kubota, Lei Li, Bin Lu, C. Mihalcea, K. Mountfield, K. Pelhos, Chubing Peng, T. Rausch, M. A. Seigler, D. Weller, and XiaoMin Yang, IEEE Trans. Magn. **42**, 2417 (2006).
[21] W. J. Carr, Jr., Phys. Rev. **109**, 1971 (1958).
[22] J. L. Garcia-Palacios and F. J. Lazaro, Phys. Rev. B **58**, 14937 (1998).
[23] R. M. Bozorth, *Ferromagnetism* (D. Van Nostrand Company, New York, 1951).
[24] D. A. Garanin and O. Chubykalo-Fesenko, Phys. Rev. B **70**, 212409 (2004).
[25] S. I. Kiselev, J. C. Sankey, I. N. Krivorotov, N. C. Emley, R. J. Schoelkopf, R. A. Buhrman, and D. C. Ralph, Nature (London) **425**, 380 (2003).
[26] Ya. B. Bazaliy, B. A. Jones, and S.-C. Zhang, Phys. Rev. B **69**, 094421 (2004).
[27] X. Jiang, L. Gao, J. Z. Sun, and S. S. P. Parkin, Phys. Rev. Lett. **97**, 217202 (2006).
[28] D. Chiba, M. Yamanouchi, F. Matsukura, T. Dietl, and H. Ohno, Phys. Rev. Lett. **96**, 096602 (2006).
[29] D. Chiba, Y. Sato, T. Kita, F. Matsukura, and H. Ohno, Phys. Rev. Lett. **93**, 216602 (2004).
[30] M. Elsen, O. Boulle, J.-M. George, H. Jaffres, R. Mattana, V. Cros, A. Fert, A. Lemaitre, R. Giraud, and G. Faini, Phys. Rev. B **73**, 035303 (2006).
[31] A. S. Núñez and A. H. MacDonald, Solid State Commun. **139**, 31 (2006).
[32] G. Grinstein and R. H. Koch, Phys. Rev. Lett. **90**, 207201 (2003).